Elevating Tessellations into Three Dimensions: Approximating Geodesic Domes

Sara Kapasi

Georgia Institute of Technology

December 2, 2021

G4G15 Gift Exchange Paper

skapasi3@gatech.edu

I. INTRODUCTION

The intrinsic and extrinsic beauty of shapes and their vast applications present themselves everywhere in our everyday lives. By combining their 3D equivalents, polyhedra, with their interlocking patterns appearing in tessellations, combining the two with both visual artistry and architectural applications in mind extends that underlying symmetry further. Integrating polyhedra and tessellations optimizes material efficiency in construction, and material efficiency in tile creation and building design in architecture is increasingly vital to sustaining a changing planet. When constructing a spherical building, many times only flat sheets of materials are available. Pouring molten metal over a cast of a building prototype is not feasible, so using small flat tiles to create the structure of a building is the closest approximation to a sphere. A sphere is ideal with its maximum volume per unit surface area, which saves on material costs. Integrating tilings provides both visual and practical appeal since making minimal cuts to create the tiles saves on cutting and gluing costs to assemble the 3D structure.

Tessellations have been present since antiquity in many designs, from the floors of the Alhambra in Spain to more recently in the works of MC Escher, the famous graphic artist and mathematician (Kaplan and Salesin 2000). They appear as the bridge between architecture and mathematics with their visual appeal and versatility (Deger and Deger 2012). A general tessellation is defined as the two-dimensional plane consisting of repeating shapes with no gaps or overlaps. Many tessellations that mathematicians work with are regular tessellations, tessellations composed solely of regular congruent polygons (Deger and Deger 2012). Semi-regular tessellations, the other class of tessellations can be made up of more than one type of shape. When constructing a tessellation, four types of transformations are used to create symmetry in the tessellation pattern. These transformations are rotations, translations, reflections, and glide reflections. One specific program used to create tessellations with the knowledge of symmetry is Microsoft Paint (Deger and Deger 2012), as well as more recent programs like Conway's Magical Pen (Bakker et al. n.d.).

When looking at polygons connected in three dimensions, polyhedra are the main focus of analysis. Polyhedra are composed of polygonal faces and their edges and vertices. These faces connect without overlap on their edges, with three faces meeting at a vertex. Convex polyhedra are generally classified into two types: Platonic solids and Archimedean solids. Archimedean solids are analogous to semi-regular tessellations, in that Archimedean solids are made up of more than one type of polygon, whereas Platonic solids are made up of one type of regular polygon (Akiyama et al. 2010).

Some of the vast appearances of polyhedra in nature include molecular structures, viruses, and various physics and architectural concepts (Koca, Al-Ajmi, and Koç 2007). However, many other applications of polyhedra extend elsewhere. In drug delivery, metal-organic polygons (MOPs) act as metallo-therapeutics which can selectively deliver drugs and dyes to tissues. Metal complexes self-assemble out of copper, palladium, platinum into structures that contribute to an inhibitory effect in tumors. The complexes sometimes assemble into tetragonal prisms, trigonal prisms, and cuboctahedron complexes, which have numerous anticancer and antitumor effects, with applications in chemotherapy and photodynamic therapy (Samanta and Isaacs 2020). Creating new polyhedra derivatives could potentially improve drug delivery efficiency through a complex able to hold more volume.

In architecture, combining Archimedean solids to create a building can reduce structural material through a unit cell. This unit cell, self-supporting and able to distribute weight equally,

is found in existing structures like the Hearst Tower in New York City and The Gherkin in London (Obradović et al. 2013). Improving this unit cell by making it more spherical can support more weight with less material. Polyhedra also have applications in sustainable water solutions as electrodes in the process of capacitive deionization. Due to the ordered and open structure of carbon nano-polyhedra, they have high permeability, which contributes to good electrochemical performance. Transmission electron microscope (TEM) and field emission scanning electron microscope (FESEM) images found the structure of the carbon nano-polyhedra to be rhombic dodecahedrons, which held their shape after multiple rounds of deionization (Xu et al. 2019). While rhombic dodecahedrons exhibit structural strength, polyhedra derivatives closer to a sphere exhibit the highest structural strength due to their likeness to a sphere, which could improve the efficiency of capacitive deionization. The durability and versatility of polyhedra in nature cannot be understated.

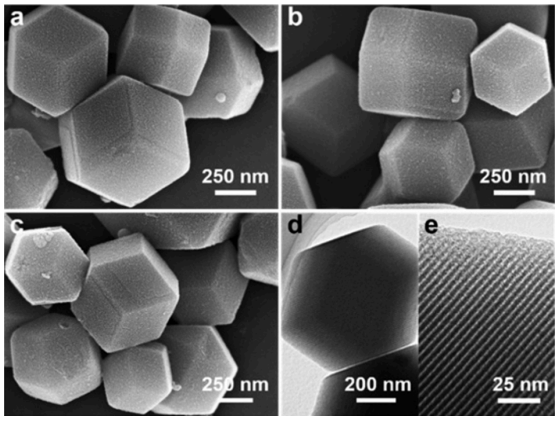

Figure 1: Carbon nano-polyhedra (Xu et al. 2019)

Figure 2: Hearst Tower, NYC ("Hearst Tower" n.d.)

Geodesic domes further complexify polyhedra, but with vast applications in architecture and material storage. The Epcot Ball at Walt Disney World, parts of the Dali Museum in Figueres, and greenhouses, are all examples of geodesic domes present in public spaces. Popularized by Buckminster Fuller, geodesic domes were based on polyhedra and had icosahedral symmetry. Subdividing their surface produced a lightweight material framework, producing triangles most commonly, but also hexagons, pentagons, and rhombi. They were applied to material systems due to their high weight-strength ratio, and Fuller was awarded multiple patents in the design and application of geodesic domes (López-Pérez 2020).

In its original context, sphericity, or "degree of true sphericity," described how close rock particles approximated a sphere (Wadell 1933) in geology. However, Wadell also hinted at sphericity's use in classifying geometric solids, signifying its cross-disciplinary usage. Wadell gives the formula for sphericity as s/S, where s is the nominal surface area of a solid (the surface area of a sphere with the same volume as the solid) and S is the actual surface area of the solid. Sphericity is an intrinsic property of a solid, or rather a dimensionless property independent of the scale of the solid due to it being a ratio with a maximum value of one. Multiple studies have used sphericity to investigate the properties of polyhedra, in the context of polyhedral complexity (Balaban and Bonchev 2005) as well as in polymer structures (Lee, Leighton, and Bates 2014). However, no studies found by the author have integrated sphericity in architectural applications.

By combining tessellations, polyhedra, and sphericity, optimizing material efficiency translates into optimizing sphericity values of polyhedra with nets of tessellations. Especially without directly renewable building materials, designing the next generation of buildings must

take into consideration material efficiency, as well as preventing unnecessary cutting or welding costs. On large scales, material inefficiency is especially hurtful towards company budgets, so designing optimal nets can redirect funds towards other crucial developments. Energy efficiency for the next generation of buildings is also needed concerning global warming, to prevent excess heat from being lost to building surroundings.

In this project, how to best approximate the net of a polyhedron with maximum sphericity using 2D tilings was investigated.

II. MATERIALS AND METHODS

The physical part of the project was split into two parts: creating the 2D tessellations and creating the 3D models. Seven tessellations were made, four of which were regular and three of which were semi-regular. To create the tessellations, Adobe Illustrator was used. Tessellations were derived by drawing in and then deleting lines of symmetry, then forming shapes around the symmetry lines with the Adobe Illustrator Polygon Tool. The command Path Length was used to find the specific centimeter side lengths, which were input into Mathematica, the program used for the 3D models. Physical copies of the tessellations were printed on cardstock and cut out using an X-Acto Knife.

For the 3D models, the objective was to elevate as many 2D tessellations as possible with the help of Mathematica. In Mathematica's integrated command library, the volume and surface area of polyhedra corresponding to the 3D models could be easily found to calculate the sphericity later. For more common polyhedra, the command PolyhedronData[], with specific commands for "SurfaceArea," "Volume," and "Net" produced the respective values for the commands listed. To ensure consistent sphericity values, the side lengths of the physical 3D models were measured and used to calculate the respective sphericity values. Adjacent to quality control, calculating the sphericity of the physical model compared to the computer model served to make sure the physical representations were accurate in assembly.

III. RESULTS AND DISCUSSION

2D Tessellations

When creating the 2D tessellations, the first class of tessellations created were the regular tessellations. Four tessellations were created, three of them qualifying as tilings since they were made up of solely regular polygons.

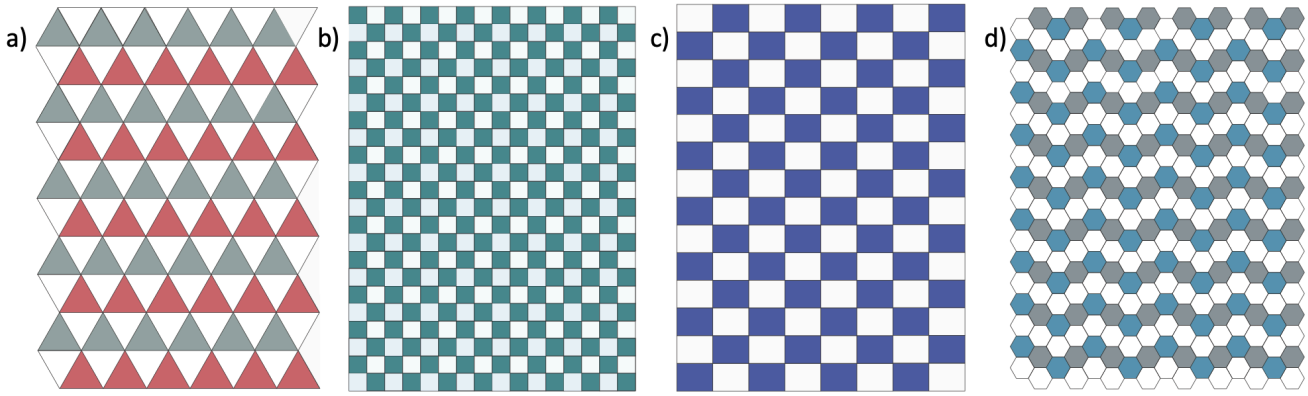

Figure 3: Regular tessellations a) Triangular tiling b) Square tiling c) Rectangular tessellation d) Hexagonal tiling

The three tilings were the triangular tiling (Figure 3a), the square tiling (Figure 3b), and the hexagonal tiling (Figure 2d), and the rectangular tessellation (Figure 3c) was included for the sake of incorporating non-regular polygons.

The second class of tessellations created were the semi-regular tessellations. Each used two colors for visibility purposes. None included solely regular polygons.

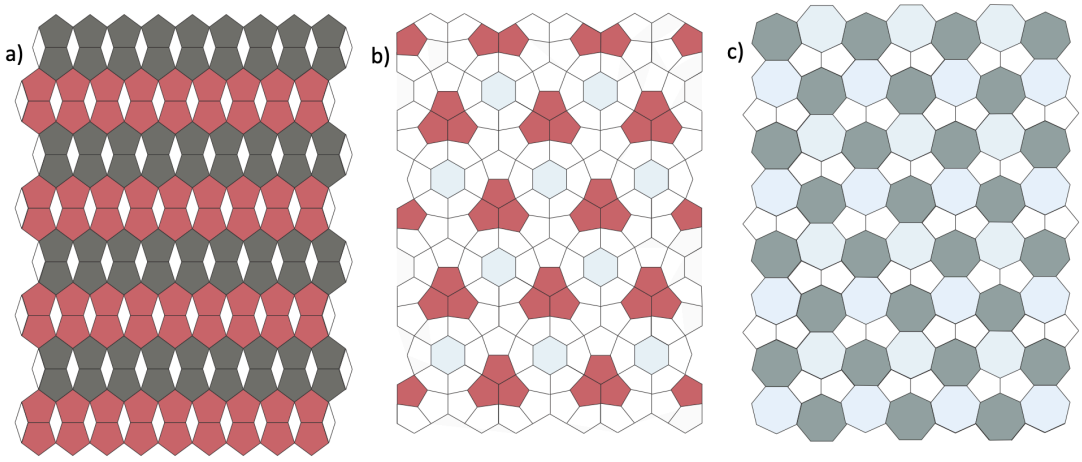

Figure 4: Semi-regular tessellations a) Pentagon-rhombus tessellation b) Pentagon-hexagon tessellation c) Pentagon-heptagon tessellation

The three semi-regular tessellations were the pentagon-rhomb tessellation (Figure 4a), the pentagon-hexagon tessellation (Figure 4b), and the pentagon-heptagon tessellation (Figure 4c).

3D Models and Corresponding Nets

When creating the 3D models, net simplicity took priority, which led to the prioritization of regular tessellations. However, due to the large interior angle of regular hexagons, the hexagonal tiling was excluded as a contender for a potential 3D model, since overlap would be inevitable when folding into 3D space. The remaining tessellations serving as nets included the triangular tiling, the square tiling, and the rectangular tessellation.

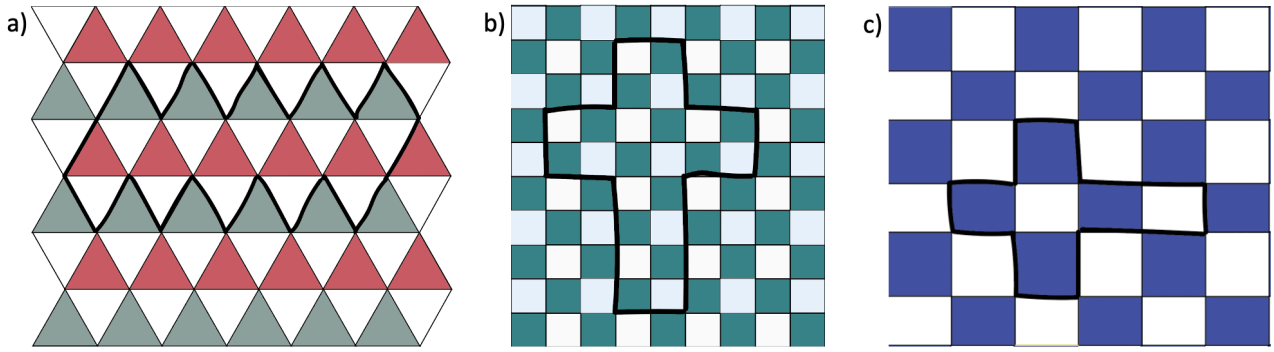

Figure 5: Potential nets directly from tessellations a) From triangular tiling b) From square tiling c) From rectangular tessellation

Icosahedron nets could be created directly from the triangular tiling (Figure 5a), and prism nets could be created directly from the square tiling (Figure 5b) and the rectangular tessellation (Figure 5c).

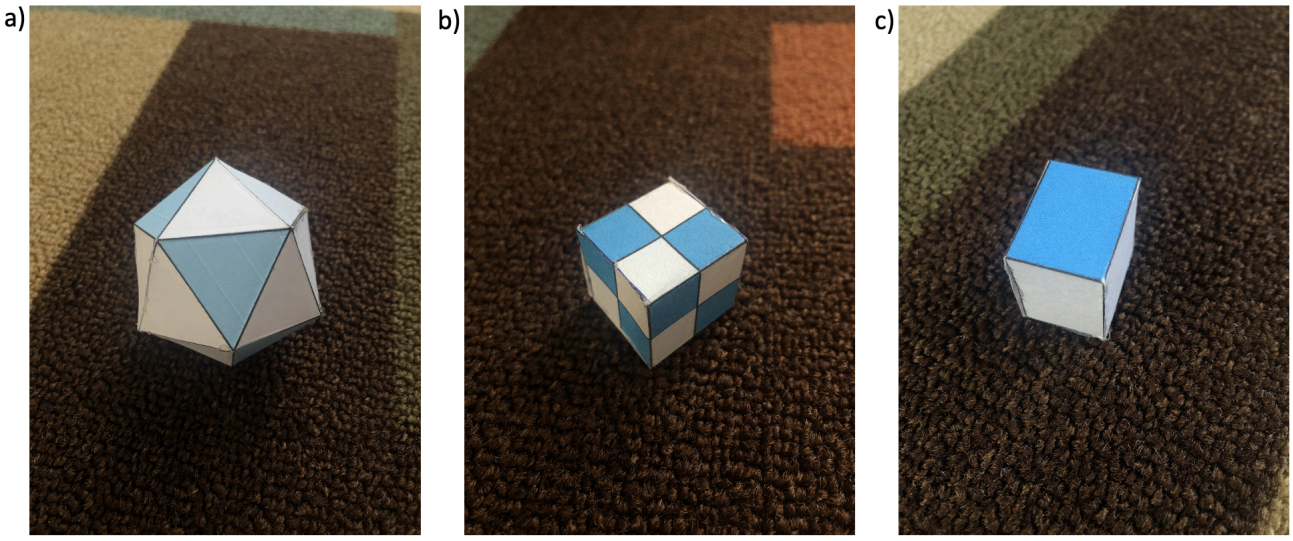

Figure 6: 3D models created directly from regular tessellations a) Icosahedron from triangular tiling b) Cube from square tiling c) Rectangular prism from rectangular tessellation

When folded upwards, the nets took the formation of an icosahedron (Figure 6a), cube (Figure 6b), and rectangular prism (Figure 6c), respectively, as predicted.

When attempting to elevate the semi-regular tessellations, three things were prioritized: the edges, center, and branches of the net. The branches are rooted in the center of the net and fold into space around each other. However, individual shapes of the net should be as connected as possible while still keeping the net in 2D. A potential net from the pentagon-heptagon tessellation was constructed, with edges to cut highlighted and branches marked in black.

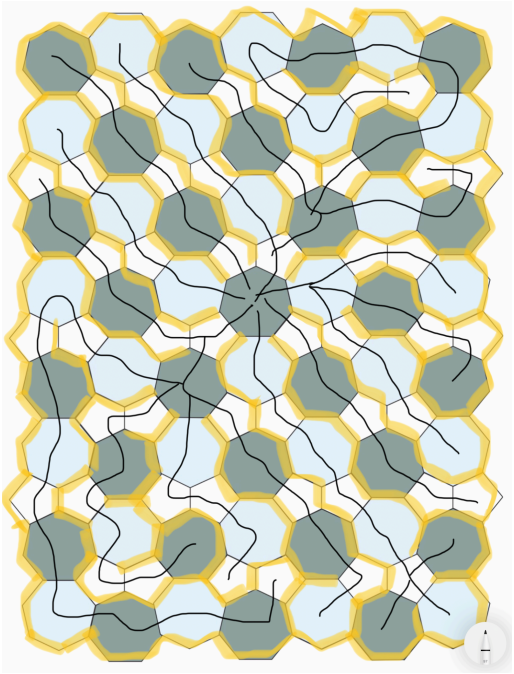

Figure 7: Pentagon-heptagon potential net, edges, and branches marked

The wings around the center of the net (Figure 7) act as supports for the surrounding wings and ideally exhibit no overlap folded upwards. However, some tessellations, including the pentagon-heptagon net, cannot directly act as nets without modification to the original tessellation, since the shapes overlap when folded upwards. By instead creating nets with the same class of shapes, rather than the same class and same configuration of shapes as the tessellation, greater flexibility for model creation appears.

To best represent the pentagon-rhomb tiling, already existing polyhedra with pentagons and triangles emerged as candidates for the approximate result of elevating a pentagon-rhomb tiling, in this case, a snub dodecahedron.

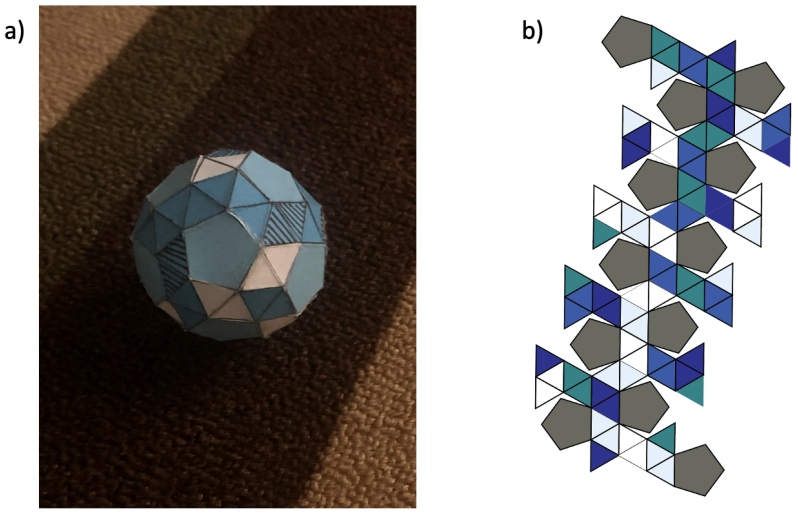

Figure 8: Snub dodecahedron a) Folded 3D model b) Color-coded net using six colors

Grouping adjacent triangles in the snub dodecahedron net (Figure 8b) by color formed rhombi of six colors so that the shape composition of the net was still pentagons and rhombi, like in the original tessellation. The choice of six colors was made to have no rhombus touching another of the same color throughout the 3D model (Figure 8a).

When elevating the pentagon-hexagon tiling, already existing polyhedra with pentagons and hexagons emerged as candidates for the approximate result of elevating a pentagon-hexagon tiling, in this case, a truncated icosahedron.

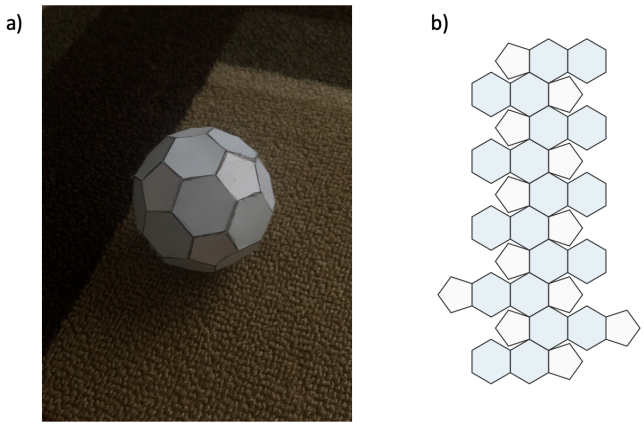

Figure 9: Truncated icosahedron a) Folded 3D model b) Color-coded net using two colors

While both the pentagon-hexagon tessellation and the truncated icosahedron model and net (Figure 9a, 9b) are made up of pentagons and hexagons, only the polygons in the truncated icosahedron are regular. Both, however, are made up of shapes with the same number of sides.

When elevating the pentagon-heptagon tiling, the existing polyhedra with pentagons and heptagons did not seem to have predicted high sphericity values. Instead, creating a novel model and the novel corresponding net emerged as a new possibility. Since the attempt to create a direct net out of the pentagon-heptagon tessellation failed, similar compromises over net space efficiency were made, like the net of the snub dodecahedron and the truncated icosahedron.

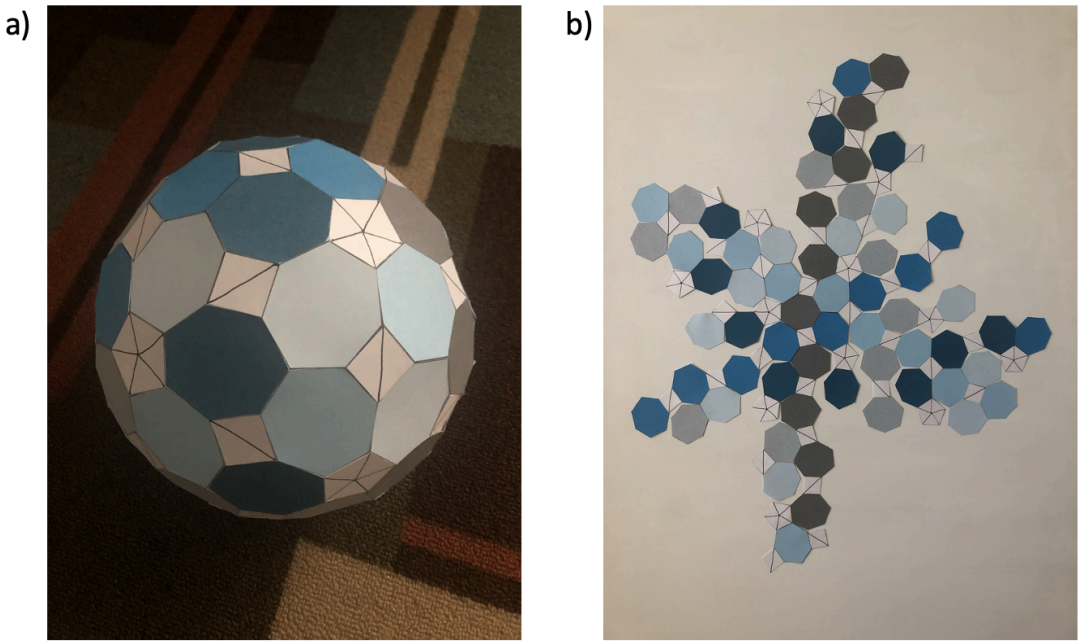

Figure 10: Novel triangle-heptagon model a) Folded 3D model b) Color-coded net using seven colors

The triangle-heptagon model (Figure 10a, 10b) has 102 faces (sixty equilateral heptagons, thirty rhombi, twelve regular pentagons), held together with hot glue. Through incorporating pentagons, the model was predicted to exhibit dodecahedral symmetry with six different “rings” around the model, leading twelve base pentagons to be used, and groups of three heptagons met at a 120º angle looking straight down. Once the model was assembled with the pentagons and heptagons, rhombus-shaped gaps appeared between the heptagons. The dimensions of the gaps were input into Adobe Illustrator and printed out for model construction usage. To keep the model limited to two types of shapes like the others, subdividing the rhombi and pentagons into triangles made the model a triangle-heptagon model, instead of a pentagon-heptagon model. Since the model was novel, surface area, volume, and thus sphericity measurements were not calculated. The known sphericity values calculated for the other models are listed below. All volume and surface area measurements were from the cm values in Adobe Illustrator.

Model	V	SA	Sphericity
Triangle	62.2115	80.8317	0.9393
Square	15.9725	38.0540	0.8060
Rectangle	12.3261	32.2964	0.7990*
Pentagon-rhombus	98.0235	104.6938	0.9820
Pentagon-hexagon	115.8653	118.9040	0.9666
Triangle-heptagon	?	?	?

Table 1: Sphericity as a function of volume (V) and surface area (SA) of the model.

Volume (V) and surface area (SA) of the model are related to sphericity (s) by the given equation $s = (\frac{3V}{4\pi})^{2/3} \times \frac{4\pi}{SA}$. The sphericity of the rectangular prism is designated by an asterisk (Table 1) since changing the side lengths of the prism changes the sphericity value, and thus a general sphericity value for a rectangular prism does not exist.

IV. CONCLUSIONS

Direct tessellations do not produce 3D models with the highest sphericity values, as the top two polyhedra with the highest sphericity values were both corresponding to semi-regular tessellations. The model with the highest calculated sphericity was the snub dodecahedron, corresponding to the pentagon-rhomb tessellation, and the model with the second-highest sphericity value was the truncated icosahedron. However, the unresolved sphericity value of the triangle-heptagon model demonstrates the triangle-heptagon model's promise as an alternative to the snub dodecahedron through its high visually-inferred sphericity. To quantify the sphericity of the triangle-heptagon model, future calculations for volume and surface area will be assessed by splitting up the model into prisms and using triple integrals to quantify the lines of symmetry pervasive through the model. Further improvement of the nets of novel models, like the triangle-heptagon model, is also needed to increase the space efficiency of the nets in the context of material sheets, since space is still present compared to the direct tessellation-derived nets. Extending this study would involve creating 2D and 3D models with different shape compositions - i.e. investigating what types of hexagons are best for tessellating, and what types of hexagons are best for elevating into polyhedra, as well as incorporating polygons with more sides, like octahedrons and dodecagons.

V. REFERENCES

1. Akiyama, Jin, Takayasu Kuwata, Stefan Langerman, Kenji Okawa, Ikuro Sato, and Geoffrey C. Shephard. 2010. “Determination of All Tessellation Polyhedra with Regular Polygonal Faces.” In *International Conference on Computational Geometry, Graphs and Applications*, 1–11. Springer. https://doi.org/10.1007/978-3-642-24983-9_1.
2. Bakker, Anton, Doris Schattschneider, Herman Tulleken, Jonathan Bailey, and Markus Krisam. n.d. “Conway’s Magical Pen.” Conway’s Magical Pen. Accessed July 25, 2021. http://conwaysmagicalpen.com/.
3. Balaban, Alexandru T., and Danail Bonchev. 2005. “Complexity, Sphericity, and Ordering of Regular and Semiregular Polyhedra.” *MATCH Communications in Mathematical and in Computer Chemistry* 54: 137–52.
4. Deger, Kubra O., and Ali H. Deger. 2012. “An Application of Mathematical Tessellation Method in Interior Designing.” *Procedia-Social and Behavioral Sciences* 51: 249–56. https://doi.org/10.1016/j.sbspro.2012.08.154.
5. “Hearst Tower.” n.d. Hearst. Accessed November 28, 2021. https://www.hearst.com/real-estate/hearst-tower.
6. Kaplan, Craig S., and David H. Salesin. 2000. “Escherization.” In *Proceedings of the 27th Annual Conference on Computer Graphics and Interactive Techniques*, 499–510. https://doi.org/10.1145/344779.345022.
7. Koca, Mehmet, Mudhahir Al-Ajmi, and Ramazan Koç. 2007. “Polyhedra Obtained from Coxeter Groups and Quaternions.” *Journal of Mathematical Physics* 48 (11): 113514. https://doi.org/10.1063/1.2809467.
8. Lee, Sangwoo, Chris Leighton, and Frank S. Bates. 2014. “Sphericity and Symmetry Breaking in the Formation of Frank–Kasper Phases from One Component Materials.” *Proceedings of the National Academy of Sciences* 111 (50): 17723–31. https://doi.org/10.1073/pnas.1408678111.
9. López-Pérez, Daniel. 2020. *R. Buckminster Fuller Pattern-Thinking*. Lars Müller Publishers.
10. Obradović, Marija, Slobodan Mišić, Branislav Popkonstantinović, Maja Petrović, Branko Malešević, and Ratko Obradović. 2013. “Investigation of Concave Cupolae Based Polyhedral Structures and Their Potential Application in Architecture.” *Technics Technologies Education Management* 8: 1198–1214.
11. Samanta, Soumen K., and Lyle Isaacs. 2020. “Biomedical Applications of Metal Organic Polygons and Polyhedra (MOPs).” *Coordination Chemistry Reviews* 410: 213181. https://doi.org/10.1016/j.ccr.2020.213181.
12. Wadell, Hakon. 1933. “Sphericity and Roundness of Rock Particles.” *The Journal of Geology* 41 (3): 310–31.
13. Xu, Xingtao, Tan Haibo, Ziming Wang, Chen Wang, Likun Pan, Yusuf Kaneti, Tao Yang, and Yusuke Yamauchi. 2019. “Extraordinary Capacitive Deionization Performance of Highly-Ordered Mesoporous Carbon Nano-Polyhedra for Brackish Water Desalination.” *Environmental Science: Nano* 6 (3): 981–89. https://doi.org/10.1039/C9EN00017H.